J Therm Anal Calorim (2010) 100:247–251
DOI 10.1007/s10973-009-0669-0

Thermal behavior and evolved gases analysis of 1,2,4-triazole-3-one derivatives

Satoru Yoshino · Atsumi Miyake

Received: 16 December 2009 / Accepted: 17 December 2009 / Published online: 7 January 2010

Abstract In order to obtain a better understanding of thermal substituent effects in 1,2,4-triazole-3-one (TO), the thermal behavior of 1,2,4-triazole, TO, as well as urazole and the decomposition mechanism of TO were investigated. Thermal substituent effects were considered using thermogravimetry/differential thermal analysis, sealed cell differential scanning calorimetry, and molecular orbital calculations. The onset temperature of 1,2,4-triazole was higher than that of TO and urazole. Analyses of evolved decomposition gases were carried out using thermogravimetry–infrared spectroscopy and thermogravimetry–mass spectrometry. The gases evolved from TO were determined as HNCO, HCN, N_2, NH_3, CO_2, and N_2O.

Keywords 1,2,4-Triazole-3-one · Thermal behavior · Evolved gas · Molecular orbital calculation

Introduction

In the recent years, the uses for energetic materials have become quite diverse and include air-bag systems, synthesis technology, and medical technology. Gas-generating agents have recently received considerable attention due to their possible applications in air-bag systems. These agents require specialized control to operate effectively. The essential features of these agents are thermal stability, the release of large volumes of gas, high combustion speed, non-explosiveness, non-toxicity (both agents and generated gas), and long-term stability [1].

The development of effective gas-generating agents by molecular design will enable the elevation of stability and control of energy release.

1,2,4-Triazole-3-one (TO; Fig. 1) contains a carbonyl group attached to a five-membered ring and is anticipated to be a useful next-generation energetic material and gas-generating agent. Previously, researchers have studied 5-nitro-1,2,4-triazole-3-one (NTO), which is equivalent in energy to 1,3,5-trinitroperhydro-1,3,5-triazine (RDX) or 1,3,5,7-tetranitroperhydro-1,3,5,7-tetrazocine (HMX), but comparatively has greater thermal stability [2–6]. Based on these characteristics, NTO is used as a propellant powder for military explosives. TO, which has a framework identical to NTO, is anticipated to exhibit greater stability and higher reactivity. The framework of the triazole ring in TO contains three nitrogen atoms; therefore, TO derivatives are expected to generate nitrogen gas during decomposition. Various sensitivities, a small-scale deflagration test, and gas generation analysis of urazole and its oxidizer compositions have been reported [7, 8]; however, the mechanism for the pyrolysis of urazole is not fully understood. In addition, there have been few detailed studies on the thermal behavior of TO. Clarification of the substituent effects of TO derivatives would enable molecular design for controlled stability and energy characteristics. In order to obtain a better understanding of substituent effects in TO derivatives, molecular orbital (MO) calculations were performed, and confirmation of the thermal behavior of TO derivatives with various numbers of carbonyl groups on the triazole ring (1,2,4-triazole, TO, and urazole; Fig. 1) and identification of the decomposition gases were investigated.

S. Yoshino (✉) · A. Miyake
Graduate School of Environment and Information Sciences, Yokohama National University, 79-7 Tokiwadai, Hodogaya-ku, Yokohama, Kanagawa 240-8501, Japan
e-mail: d07tf010@ynu.ac.jp

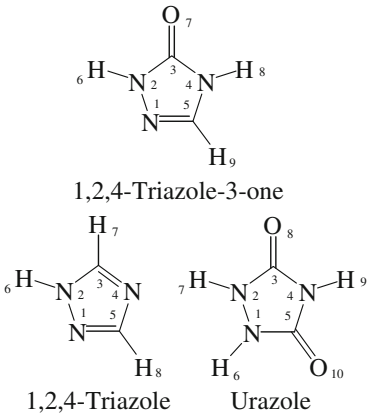

Fig. 1 Numbering schemes and molecular structures of 1,2,4-triazole, TO, and urazole

Experimental

Agents

TO was obtained and confirmed by employing a previously reported method [9, 10]. Reagent grade purity 1,2,4-triazole (98%, Tokyo Kasei Kogyo Co., Ltd.) and urazole (97%, Kanto Chemical Co., Inc.) were used without further purification.

Instruments

Molecular orbital calculations were performed using the Gaussian 03 program [11]. Geometric optimization of the structures and vibration analyses were achieved within the framework of density functional theory (DFT) using the B3LYP method at the level of 6-311++G(d,p) (restricted closed-shell).

The thermal properties were analyzed by thermogravimetry/differential thermal analysis (TG/DTA; Shimadzu Co. Ltd., DTG-50) under an argon gas flow rate of 20 mL min^{-1}. Samples (2 mg) were measured in an aluminum pan at a heating rate of 10 K min^{-1} in the range of 25–500 °C. Sealed cell-differential scanning calorimetry (SC-DSC; Mettler Toledo, HP DSC827e) was carried out for samples (1 mg) in a stainless steel sealed cell (Seiko Instruments Inc.) at a heating rate of 10 K min^{-1} over the measurement range of 25–500 °C. In order to estimate the apparent activation energy (E_a) for thermal decomposition, SC-DSC was carried out at different heating rates (1, 3, 5, 10, and 15 K min^{-1}), and Ea was estimated by the Kissinger method using the exothermic peak temperatures. Infrared spectroscopy (JOEL, FT/IR-420) was used for structural confirmation of TO residues.

Thermogravimetry–infrared spectroscopy (TG–IR) was used to identify the decomposition gases evolved from the pyrolysis of TO. The apparatus consisted of two parts: TG (Shimadzu Co., DTG-50) and an IR spectrometer (Shimadzu Co. Ltd., IRPrestige-21). The gases evolved after pyrolysis of the samples (3 mg) by TG were fed to a gas cell for IR analysis through a stainless steel transfer line. TG–IR was carried out using a pin-hole aluminum pan under an argon gas flow of 20 mL min^{-1} with the following conditions: heating rate, 95 K min^{-1}; measurement range, room temperature (RT; 25-30 °C)–500 °C; transfer line and IR gas cell temperature, 200 °C; scanning resolution, 8 cm^{-1}. The spectra were integrated 15 times.

Thermogravimetry–mass spectrometry (TG–MS) was employed for real-time analysis of the gas evolved from TO pyrolysis. The TG–MS apparatus consisted of two parts: TG (Rigaku Co., TG8120) and a mass spectrometer (Shimadzu Co., GCMS-QP2010). TG–MS was carried out using a pin-hole aluminum pan under a helium gas flow of 200 mL min^{-1} with the following conditions: heating rate, 95 K min^{-1}; measurement range, RT–500 °C; oven temperature, 200 °C. The components of the evolved gases were identified on the basis of IR and MS reference spectra, available in the spectral libraries of the National Institute of Standards and Technology (NIST) and from a previous study [12].

Results and discussion

Molecular orbital calculations

The bond lengths and angles for the geometric optimization of structures calculated at the B3LYP/6-311++G(d,p) level are presented in Table 1. Both the geometries of 1,2,4-triazole and TO indicated planar structures. 1,2,4-Triazole, which satisfies Huckel's rule, is known to exhibit aromaticity and a planar structure. Since TO, which does not satisfy Huckel's rule, was also found to have planar structure, TO is expected to have aromatic characteristics. Urazole did not have a planar structure, because the bonds of the triazole ring are thought to become σ-bonds, due to the presence of two carbonyl groups. Furthermore, the length of the N1–N2 bond was increased with the number of carbonyl groups on the triazole ring, and the angles were changed with the bond length. Therefore, the bond lengths of the 1,2,4-triazole, TO, and urazole were influenced by the substituents on the triazole ring.

Thermal analysis

TG/DTA curves for the 1,2,4-triaozle, TO, and urazole are shown in Fig. 2. At 228 °C, an endothermic peak in the DTA curve and a loss of mass in the TG curve were observed. The TG curve of TO indicates that the mass loss is one-step. The DTA curve has two endothermic peaks at 239 and 275 °C.

Table 1 Geometric structures of 1,2,4-triazole, TO, and urazole at the B3LYP/6-311++G(d,p) levels

TO		1,2,4-Triazole		Urazole	
Bond	Length/Å	Bond	Length/Å	Bond	Length/Å
N1–N2	1.376	N1–N2	1.355	N1–N2	1.426
N2–C3	1.380	N2–C3	1.322	N2–C3	1.404
C3–N4	1.402	C3–N4	1.364	C3–N4	1.390
N4–C5	1.375	N4–C5	1.318	N4–C5	1.390
N2–H6	1.006	N1–H6	1.008	N1–H6	1.014
C3–O7	1.213	C3–H7	1.079	N2–H7	1.014
N4–H8	1.007	C5–H8	1.079	C3–O8	1.204
C5–H9	1.078			N4–H9	1.008
				C5–O10	1.204
TO		1,2,4-Triazole		Urazole	
Bond	Angle/°	Bond	Angle/°	Bond	Angle/°
N1–N2–C3	114.22	N1–N2–C3	101.99	N1–N2–C3	107.86
N2–C3–N4	100.89	N2–C3–N4	115.08	N2–C3–N4	104.75
C3–N4–C5	108.79	C3–N4–C5	102.90	C3–N4–C5	112.69
N4–C5–N1	112.00	N4–C5–N1	109.77	N4–C5–N1	104.75
N1–N2–H6	120.31	N1–N2–H6	120.03	N1–N2–H7	113.39
N2–C3–O7	130.19	N2–C3–H7	121.69	N2–C3–O8	113.39
C3–N4–H8	123.23	N4–C5–H8	126.65	C3–N4–H9	126.84
N4–C5–H9	123.98			N4–C5–O10	123.66
				C5–N1–H6	128.41

From a previous study [10], it was thought that the mass loss TO exhibits by the first endothermic peak was due to melting of TO. Figure 3 shows the DSC curves of 1,2,4-triazole, TO, and urazole. Following the endothermic peaks indicating melting in the DSC curves, exothermic peaks indicating decomposition were also observed.

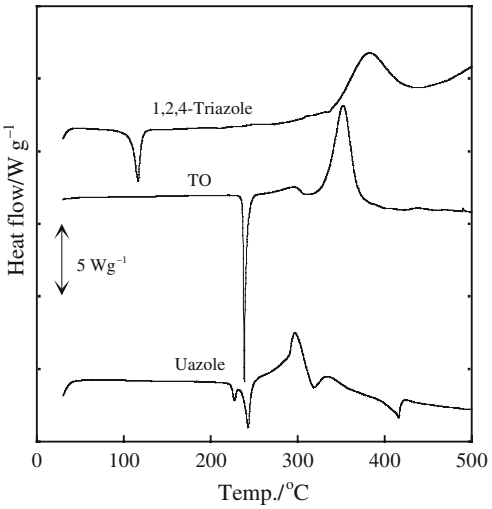

Fig. 3 DSC curves of 1,2,4-triazole, TO, and urazole derivatives in sealed SUS cell at a heating rate of 10 K min^{-1}

The difference between the thermal behavior of TO observed in the TG/DTA and SC-DSC results was due to the different measurement conditions. While the exothermic peak in the DSC curve indicates the decomposition of TO, the second endothermic peak of the DTA curve indicates the vaporization of TO. In order to investigate this cause, SC-DSC measurement of TO with sealed aluminum cell was carried out using two measurement temperatures (300 and 400 °C), and the residue of TO was analyzed by IR measurement using the KBr method (Fig. 4). The IR spectra of the TO residue at RT and at 300 °C showed a slight difference. However, there were also differences between the IR spectral shapes of the residue at 400 °C and those of RT and

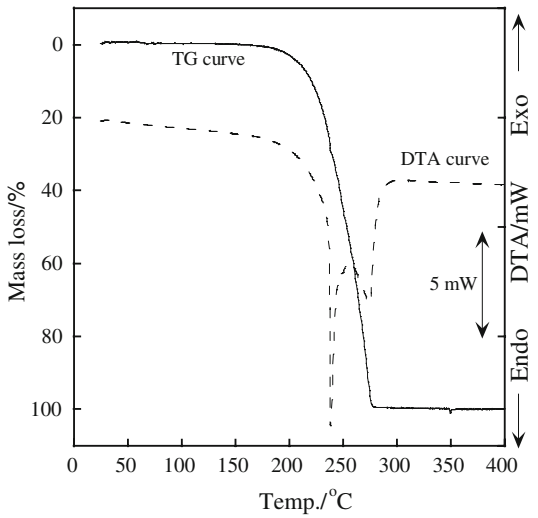

Fig. 2 TG/DTA curves of TO in aluminum pan at a heating rate of 10 K min^{-1}

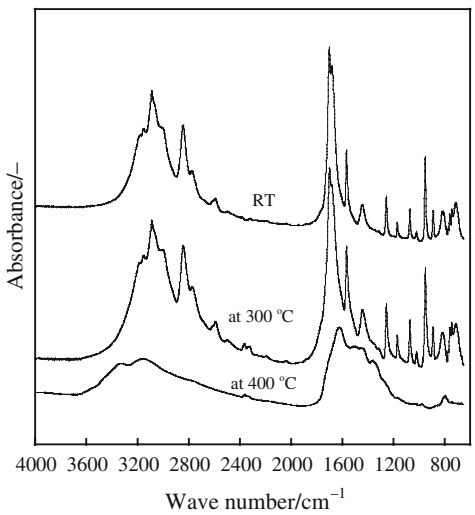

Fig. 4 IR spectra of TO residues of various temperatures (RT, 300, 400 °C)

Table 2 Results of thermal analysis and MO calculations of 1,2,4-triazole, TO, and urazole

Sample	Bond length N1–N2/Å	m.p./ °C	T_{tg}/ °C	T_{dsc}/ °C	Q_{dsc}/ J g^{-1}	E_a/ kJ mol^{-1}
1,2,4-Triazole	1.36	113	100	341	1028	148
TO	1.38	236	197	332	1043	158
Urazole	1.43	222	220	254	935	162

at 300 °C. Furthermore, the unsealed measurement exhibited endothermic peaks, and no residue remained after TG/DTA was performed on TO; however, for the sealed cell measurement, exothermic peaks were observed. Comparison of these results suggests that TO decomposes in the gas phase after melting and vaporization.

The thermal analysis results in Table 2 summarizes melting points (m.p.), initiation temperatures of mass loss (T_{TG}) by TG, onset temperatures (T_{DSC}) by SC-DSC, heat of decomposition (Q_{DSC}) by SC-DSC, and apparent E_a for thermal decomposition, which was estimated by the Kissinger method using the exothermic peak temperatures from SC-DSC results at different heating rates (1, 3, 5, 10, 15 K min^{-1}).

The numbers of carbonyl groups were found to have an influence on T_{TG} and T_{DSC}. When the numbers of carbonyl groups on the triazole ring increased, T_{DSC} decreased, and T_{TG} and E_a were increased. From MO calculations, the length of the N1–N2 bond increased with increasing number of carbonyl groups on the triazole ring. Urazole does not have a planar structure, because the number of π-bonds in the triazole ring decreases with the increasing number of carbonyl groups on the triazole ring, so that the triazole ring loses aromaticity; the T_{DSC} of urazole was less than the 1,2,4-triazole and TO. Therefore, carbonyl groups on the triazole ring contribute to the geometric structure and thermal stability, and these triazole ring substituent effects are expected to have an effect on thermal stability.

Gas evolved from TO

Thermal analysis indicates that TO is decomposed in the gas phase after melting and vaporization. Therefore, in order to determine the cause of decomposition for TO, TG–IR and TG–MS were carried out at a heating rate of 95 K min^{-1}. For identification of gases evolved from TO, the IR spectrum of TO at 500 °C is shown in Fig. 5. The signals observed were νCO_2: 2300–2400 cm^{-1}, νHNCO: 2250–2275 cm^{-1}, νHCN: 3200–3350 cm^{-1}, νN_2O: 2225 cm^{-1}, νC=O, νNH_3: 1500–1600 cm^{-1}, and δNH_3: 950 cm^{-1}. From these results, it was determined that the decomposition gases evolved from TO at 500 °C were HNCO, HCN, NH_3, CO_2, and N_2O.

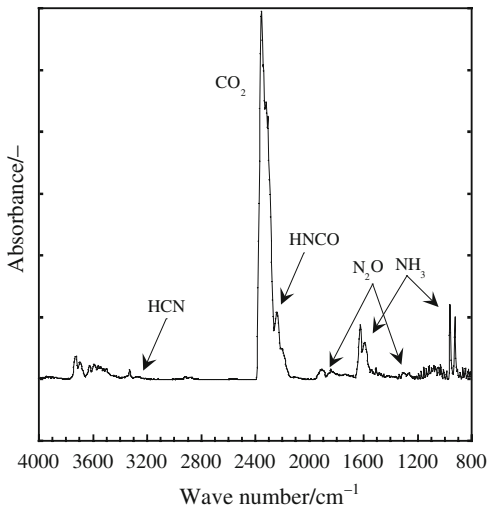

Fig. 5 IR spectrum of gases evolved from TO using TG–IR at a heating rate of 95 K min^{-1}

Real-time analysis of the evolved gas was carried out using TG–MS. Gases evolved from a sample (3 mg) was fed through a capillary to the ion source of the mass spectrometer, and analyzed by electron impact ionization. Figure 6 shows the MS spectrum of gases evolved from TO during the first 3.6–4.9 min (369–507 °C). HNCO, CO_2, N_2O, HCN, NH_3, and N_2 were identified from their characteristic peaks, and these results are in agreement with the TG–IR results. In addition, it was found that the mass-to-charge ratio (m/z) = 43 peak of HNCO exhibited the highest intensity. Figure 7 shows the mass loss of TO and intensity curves of m/z = 43(HNCO) and m/z = 17(NH_3 etc.) fragments by TG–MS as a function of time. The first peaks in the mass spectra were observed during the first 3.6 to 4.9 min. From 4.9 to 6.8 min, secondary peaks were

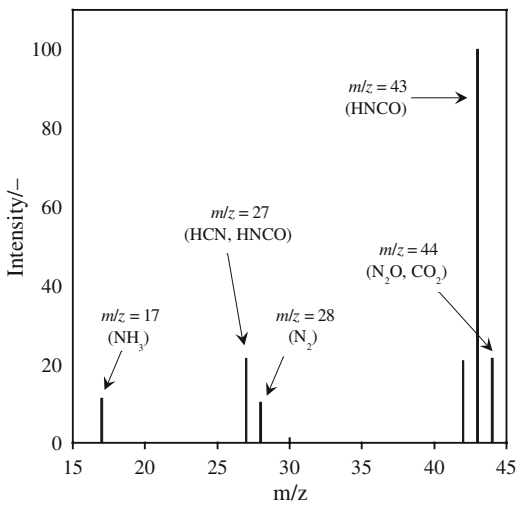

Fig. 6 MS spectrum of gases evolved from TO using TG–MS at a heating rate of 95 K min^{-1}

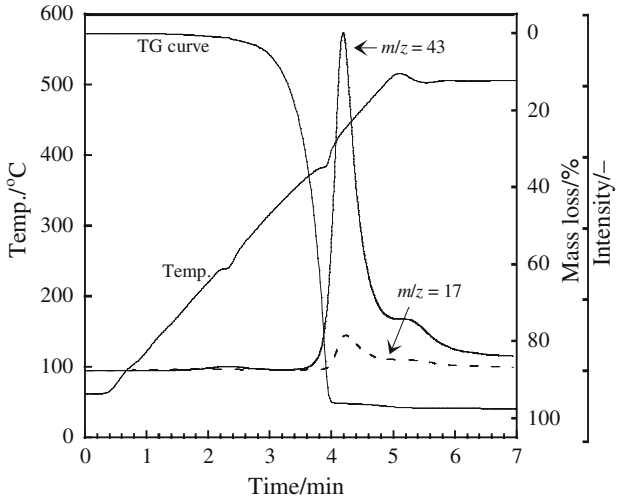

Fig. 7 TG and intensity curves of gases evolved from TO ($m/z = 43$, 17) using TG–MS at a heating rate of 95 K min^{-1}

observed. It was considered that the decomposition of the TO residue resulted in these secondary peaks. The HNCO fragments ($m/z = 43$) appear at the leading edge (3.6 min), and the NH_3 fragment ($m/z = 17$) appeared at 4.0 min. Therefore, the arrival time of NH_3 ($m/z = 17$) was later than that of HNCO ($m/z = 43$). It has been reported that CO_2 and NH_3 gases are produced by the decomposition of HNCO at temperatures higher than 80 °C [12]. From these results, it was assumed that the NH_3 gas was a decomposition product of the evolved gases.

Discussion of initial decomposition mechanism

A mechanism for the initial decomposition of TO was considered from the results of the evolved gas analysis. HNCO exhibited the highest intensity and was the first peak to appear; therefore, two paths are considered for the production of HNCO from TO. The first path is the dissociation of the N1–N2 and C3–N4 bonds in the TO structure. The second path is the dissociation of the N2–C3 and N4–C5 bonds. According to the MO calculations for TO, the length of the C3–N4 bond was longer than the others in the optimized TO structure. Therefore, the proposed mechanism for the initial decomposition of TO is ring-opening (C3–N4 and N1–N2 bonds) of the triazole ring.

Conclusions

Based on the experimental investigation of thermal substituent effects in 1,2,4-triazole, TO, urazole, and the mechanism determined for the thermal decomposition of TO, the following conclusions can be drawn:

(1) The presence of carbonyl groups in the TO derivatives has a significant influence on the thermal stability of the structures.
(2) The gases evolved from TO at 500 °C were HNCO, HCN, N_2, NH_3, CO_2, and N_2O.
(3) HNCO was evolved as the major gas for the thermal decomposition of TO.
(4) NH_3 gas was a product of the decomposition of evolved gases.
(5) Ring-opening of the triazole ring is proposed as the mechanism for the initial decomposition of TO.

References

1. Tamura M, Arai M, Akutsu Y. Energetic material and safety. Tokyo: Asakura Shoten; 1999. (Japanese).
2. Hara Y, Taniguchi H, Ikeda Y, Takayama S, Nakamura H. The thermal decomposition and hazards evaluation for 3-nitro-1, 2, 4-triazol-5-one. Sci Technol Energ Mater. 1994;55:183–7.
3. Thangadurai S, Karatha KPS, Sharma DR, Shukla SK. Review of some newly synthesized high energetic materials. Sci Technol Energ Mater. 2004;65:215–26.
4. Rothgery EF, Audette DE, Wedlich RC, Csejka DA. Preparation, crystal structure, thermal decomposition mechanism, and thermodynamical properties of $H[Pr(NTO)_4(H_2O)_4]_2{\cdot}H_2O$. Thermochim Acta. 1991;185:19–25.
5. Spear RJ, Louey CN, Wolfson MG. MRL technical report. MRL TR-89-18. 1989.
6. Sinditskii VP, Smirnov SP, Egorshev VY. Thermal decomposition of NTO: an explanation of the high activation energy. Propellants Explos Pyrotech. 2007;32:277–87.
7. Arai M, Tsukahara T, Ueda Y, Ichikawa K, Tamura M. Some properties of triazoles and their compositions—as candidates for new gas generating agent of the air bag system. Proceedings of 23th international pyrotechnics seminar, Tsukuba, September 30–October 4, 1997. p. 53–63.
8. Arai M, Tsukahara T, Tamura M. Deflagration properties of triazoles and their compositions—as candidates for new gas generating agent of the air bag system. Proceedings of 26th international pyrotechnics seminar, Nanjing, October 1–4, 1999. p. 7–14.
9. Haines DR, Leonard NJ, Wiemer DF. Syntheses and structure assignments of six azolinone ribonucleosides. J Org Chem. 1982; 47:474–82.
10. Yoshino S, Ihara S, Matsunaga K, Miyake A. Synthesis and thermal behavior of 2,4-diaryl-3H-1,2,4-triazole-3-ones. Sci Technol Energ Mater. 2009;70:16–22.
11. Frisch MJ, Trucks GW, Schlegel HB, Scuseria GE, Robb MA, Cheeseman JR, et al. Gaussian 03 Revision E 01. Wallingford: Gaussian Inc.; 2004.
12. Fischer G, Geith J, Klapotke TM, Krumm B. Synthesis, properties and dimerization study of isocyanic acid. Z Naturforsch. 2002;57b:19–24.